



Contents lists available at ScienceDirect

Nuclear Inst. and Methods in Physics Research, A

journal homepage: www.elsevier.com/locate/nimaGrowth and luminescent properties of new Eu^{2+} doped RbBa_2I_5 scintillatorN.V. Rebrova^{a,*}, A.Yu. Grippa^a, R. Calà^{b,c}, L. Martinazzoli^{b,c}, E. Auffray^c, I.A. Boiaryntseva^a^a Institute for Scintillation Materials, National Academy of Sciences of Ukraine, Nauky Avenue 60, 61072 Kharkov, Ukraine^b Università degli Studi di Milano-Bicocca, Italy^c CERN, EP department, Geneva, Switzerland

ARTICLE INFO

Keywords:

RbBa₂I₅

Inorganic materials

Crystal growth

Optical properties

X-ray and gamma-ray spectroscopies

ABSTRACT

A novel crystal scintillator of $\text{RbBa}_2\text{I}_5:\text{Eu}^{2+}$ was grown by the Bridgman–Stockbarger method. Its luminescence and scintillation properties were investigated. Under X-ray excitation, the crystal demonstrates blue luminescence peaking at 436 nm associated with $4f^65d^1 \rightarrow 4f^7$ radiative transitions of Eu^{2+} ions. The main X-ray luminescence decay constant is 800 ns. The light output of $\text{RbBa}_2\text{I}_5:3\%\text{Eu}^{2+}$ sample under 662 keV excitation is 58,200 ph/MeV.

1. Introduction

Research on luminescent materials activated by rare earth ions is very active. The studied luminescent materials can be classified as either storage phosphors or scintillators. While the storage phosphors accumulate the incident radiation energy in a form of carrier trapping, the scintillators convert a high energy ionizing radiation to visible photons via energy transfer from the host matrix to emission centers. Scintillation materials have application in various fields such as in security, dosimetry, high energy physics and medical imaging.

The most extensively used scintillators are NaI:Tl and CsI:Tl [1,2], which show good light yield and are easily grown in large sizes. In search of an alternative to them, much attention was paid to materials based on alkaline earth (Ca, Sr, Ba) di-iodides activated with Eu^{2+} , which demonstrate better scintillation performance [3–5]. Indeed, the light yield of $\text{SrI}_2:\text{Eu}^{2+}$ and $\text{CaI}_2:\text{Eu}^{2+}$ crystals is almost three times higher than for NaI:Tl [3]. At the same time, despite excellent scintillation characteristics, difficulties arise with their practical application due to their high hygroscopicity. In addition, $\text{CaI}_2:\text{Eu}^{2+}$ has a layered structure.

Progress in engineering of scintillators imposes new requirements on materials and continues to drive the search for “new generation” of scintillators. One of the contenders is the family of compounds, which can be represented by the generic chemical formula $\text{AB}_2\text{I}_5:\text{Eu}^{2+}$ (A = alkali metals; B = alkaline earth metals). It has been reported that Sr-containing compounds of the series, namely $\text{KSr}_2\text{I}_5:\text{Eu}^{2+}$ and $\text{RbSr}_2\text{I}_5:\text{Eu}^{2+}$, show a light yield of ~ 90,000 ph/MeV with an energy resolution of less than 3% [6,7]. Rb has not always been considered in scintillator composition, since it includes 27.8% of the ^{87}Rb isotope, which gives a relatively high level of background radioactivity. But

despite the presence of the ^{87}Rb isotope, which undergoes beta-decay to ^{87}Sr with the emission of an electron with end-point energy of 282 keV, the detection of gamma-rays with energies above 283 keV remains unaffected [8].

The crystals with Ba are also very promising scintillators with a light yield of 90,000 ph/MeV for $\text{KBa}_2\text{I}_5:\text{Eu}^{2+}$ [9] and 102,000 ph/MeV for $\text{CsBa}_2\text{I}_5:\text{Eu}^{2+}$ [10]. The best energy resolution values are 2.4% and 2.55%, respectively [9,10]. In addition, $\text{CsBa}_2\text{I}_5:\text{Eu}^{2+}$ and $\text{KSr}_2\text{I}_5:\text{Eu}^{2+}$ are less hygroscopic compared to $\text{SrI}_2:\text{Eu}^{2+}$ [6,10]. Therefore, they have good potential for competition with $\text{SrI}_2:\text{Eu}^{2+}$.

In this work, we report on the new scintillation material $\text{RbBa}_2\text{I}_5:3\%\text{Eu}^{2+}$, which belongs to the series described above. It crystallizes in monoclinic space group $\text{P}2_1/c$ (14) with unit cell parameters $a = 10.36 \text{ \AA}$, $b = 9.257 \text{ \AA}$, $c = 14.74 \text{ \AA}$, $\beta = 90.356^\circ$; its density is 4.667 g/cm^3 [11,12]; $Z_{eff} = 52.94$ (calculated by formula [13]). The research presented in this paper is focused on crystal growth, luminescence and scintillation properties of $\text{RbBa}_2\text{I}_5:3\%\text{Eu}^{2+}$.

2. Experimental

The single crystals of $\text{RbBa}_{2-x}\text{Eu}_x\text{I}_5$ ($x=0$ and 0.3) were prepared from mixtures of the individual components RbI (99.9%), BaI_2 and EuI_2 (99.99%) taken in stoichiometric ratios. The anhydrous starting iodide of BaI_2 was previously synthesized from BaCO_3 (99.99%) powder.

BaI_2 was synthesized by the following reaction:



Water was added to the calculated amounts of BaCO_3 and I_2 . Hydrazine solution was then added dropwise during 2 h to the stirred mixture.

* Corresponding author.

E-mail address: nadindr1985@mail.ru (N.V. Rebrova).

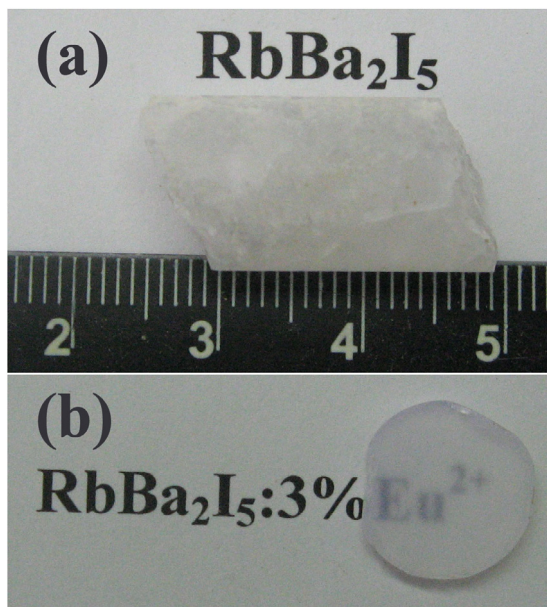


Fig. 1. Undoped RbBa_2I_5 crystal (a) and polished $\text{RbBa}_2\text{I}_5:3\%\text{Eu}^{2+}$ sample of 3 mm thickness (b).

When the reaction was completed, the resulting mixture ceased to bubble and turned colorless. The flask with the solution was heated to boiling. As the water evaporated, the mixture became supersaturated and crystals of $\text{BaI}_2 \times n\text{H}_2\text{O}$ started to form. Then, NH_4I was added to wet $\text{BaI}_2 \times n\text{H}_2\text{O}$ and mixed well in a mortar. The solid mixture was dehydrated in vacuum to 480°C with a heating rate of $10^\circ\text{C}/\text{h}$ until the NH_4I completely sublimated and anhydrous BaI_2 formed.

The charge preparation and all manipulations with the obtained crystals were carried out in a glove box. The single crystals of RbBa_2I_5 and $\text{RbBa}_2\text{I}_5:3\%\text{Eu}^{2+}$ were grown in evacuated and sealed quartz ampoules using the Bridgman–Stockbarger method. To reduce adhesion, ampoules coated with pyrolytic carbon were used.

The charged sealed ampoule was transferred to a crystal growth furnace. The ampoule was heated until the charge was melted. To provide good mixing of the components and complete the formation of $\text{RbBa}_{2-x}\text{Eu}_x\text{I}_5$ ($x=0, 0.3$), the ampoule was kept at this temperature for 24 h. The final step of the crystal growth procedure was the pulling down of the ampoule with the melt from a high temperature zone to a low temperature zone through a temperature gradient of $10^\circ\text{C}/\text{cm}$ with a pulling rate of 1.5 mm/h. When the crystal growth had gone to completion, the ampoule in the furnace was cooled to room temperature with a cooling rate of $7^\circ\text{C}/\text{h}$. Then, the ampoule was removed from the furnace and the obtained crystal was extracted by cutting the ampoule with a diamond cut off wheel.

The grown crystals of RbBa_2I_5 and $\text{RbBa}_2\text{I}_5:3\%\text{Eu}^{2+}$ were opaque (see Fig. 1). The grown boules had many cracking (Fig. 1a), but no inclusions were observed. The boules were cut with a diamond cut off wheel to $\varnothing 8 \times 3$ mm slabs (Fig. 1b). The obtained slabs were polished with diamond lapping powders (7–40 μm) and sealed in aluminum housing. A 3M-ESR polymer film was used as a reflector.

To evaluate the hygroscopicity, fresh samples of $\varnothing 12 \times 2$ mm were cut off from the boules, and their weight gain in atmospheric air versus time was measured. The measurements on the unpolished samples were carried out at room temperature. The relative humidity of the air was $40\% \pm 2\%$.

Luminescence and kinetic measurements were carried out in reflectance mode using a combined fluorescence lifetime and steady-state spectrometer FLS 920 (Edinburgh Instruments) equipped with a xenon Xe 450 W lamp for steady-state measurements and hydrogen

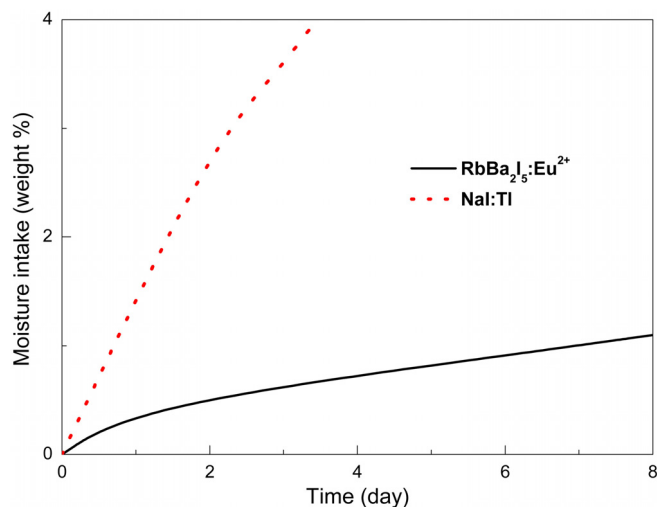


Fig. 2. Hygroscopic nature of $\text{RbBa}_2\text{I}_5:\text{Eu}^{2+}$ as compared to NaI:Tl under a temperature of 22°C and relative humidity of $40 \pm 2\%$.

filled nF 900 nanosecond flashlamp for time correlated single photon counting measurements. Photoluminescence excitation spectra were corrected on the incident photon flux. Photoluminescence emission spectra were corrected for the spectral sensitivity of the detection system.

Radioluminescence spectra were recorded under steady-state X-ray excitation (Cu anode, 40 kV, 40 μA) at 300 K. Emitted light was dispersed using a monochromator equipped with a 1200 grooves/mm grating and was recorded with a Hamamatsu R1926A PMT.

Scintillation light output was measured on the $\varnothing 8 \times 3$ mm housed sample under a ^{137}Cs gamma-ray source. The set-up consisted of a Hamamatsu R2059 PMT connected to a CAEN digitizer DT5720A through an analog attenuator employed to avoid saturation. The test bench calibration was based on the measurement of the signal produced by a single photoelectron escaping the photocathode as in [14]. An integration gate of 16 μs was used. The sample of $\text{RbBa}_2\text{I}_5:3\%\text{Eu}^{2+}$ was coupled to the photocathode with glycerine as optical coupling. A gamma radiation source was placed on top of the sample. The instrumental error in the measurement was estimated to be 5%.

Scintillation decay times were determined under pulsed X-ray excitation (35 kHz excitation repetition rate) using a Hamamatsu N5084 light-excited X-ray tube (30 kV) with a Hamamatsu PLP-10 picosecond light pulser as an optical excitation source. The scintillation decay was registered by PMA 165-6 PMT from PicoQuant operating in a single photon counting mode.

3. Results and discussion

The effect of atmospheric humidity on the moisture intake by crystals with dimension of $\varnothing 12 \times 2$ mm is shown in Fig. 2. As a reference, the uptake of a NaI:Tl crystal with the same size was recorded. The amount of moisture absorbed by $\text{RbBa}_2\text{I}_5:\text{Eu}^{2+}$ is significantly lower than that of the reference. In [9], the crystal of $\text{KBa}_2\text{I}_5:4\%\text{Eu}^{2+}$ shows a moisture sorption level close to NaI:Tl . Compared with these data, it is clear that the $\text{RbBa}_2\text{I}_5:\text{Eu}^{2+}$ crystal is less hygroscopic than $\text{KBa}_2\text{I}_5:4\%\text{Eu}^{2+}$. After the moisture absorption experiment, the $\text{RbBa}_2\text{I}_5:\text{Eu}^{2+}$ crystal remained the same size, but the external surfaces turned white. The crystal can be restored to a pristine condition by polishing the damaged surface.

Fig. 3 shows the X-ray excited emission spectra of $\text{RbBa}_{2-x}\text{Eu}_x\text{I}_5$ ($x=0$ and 0.3) crystals at 300 K. For $\text{RbBa}_2\text{I}_5:3\%\text{Eu}^{2+}$, a single luminescence peak at 436 nm corresponds to $4f^6 5d^1 \rightarrow 4f^7$ radiative transitions of Eu^{2+} ions [15]. In the case of undoped RbBa_2I_5 , X-ray excited

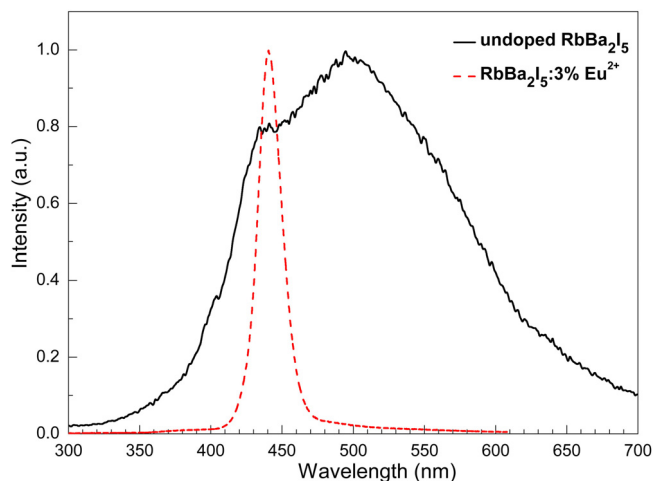


Fig. 3. X-ray excited emission spectra of $\text{RbBa}_{2-x}\text{Eu}_x\text{I}_5$ ($x=0$ and 0.3) crystals at 300 K.

emission spectrum represents a superposition of emission bands with maxima around 430 and 500 nm.

The excitation spectrum for 430 nm emission of the undoped RbBa_2I_5 crystal (see Fig. 4a) reveals two sets of bands centered at 285 and 335 nm and a strong excitation band with a maximum near 255 nm. Excitation in the 285–370 nm range is attributed to $4f^7 \rightarrow 4f^65d^1$ transitions of Eu^{2+} ions and gives rise to typical emission peaking at 428 nm. Small traces of Eu^{2+} are present in the undoped crystal due to europium contamination of the vacuum system during earlier sample preparation of other systems of europium-containing crystals. In the case of $\text{RbBa}_2\text{I}_5:3\%\text{Eu}^{2+}$, the luminescence maximum is shifted toward a longer wavelength and is located at 432 nm (Fig. 4b) due to the well-known self-absorption effect [16,17] (a significant overlap between the excitation and emission spectra is clearly seen in Fig. 4b).

In the luminescence spectra of the RbBa_2I_5 crystals, only one type of Eu^{2+} emission centers is observed. This result correlates with theoretical calculations in which Eu^{2+} preferentially occupies sevenfold coordinated Ba^{2+} sites in ABa_2I_5 ternary halides [18].

A broad emission band centered at 500 nm is observed under X-ray and photo excitation at 255 nm in the undoped RbBa_2I_5 (Fig. 4a). A similar long-wave luminescence was also reported for SrI_2 [3], BaI_2 [19], CsBa_2I_5 [17] and was ascribed to the creation of impurity-trapped excitons [17]. In $\text{RbBa}_2\text{I}_5:3\%\text{Eu}^{2+}$, this long-wave emission is suppressed.

Fig. 5a depicts two decay time profiles for the undoped RbBa_2I_5 crystal at 300 K. The decay time profile for 428 nm emission under excitation at 335 nm is single-exponential with a time constant of about 380 ns. This value is in good agreement with 360 ns radiative lifetime of Eu^{2+} $4f^65d^1$ excited state in the “undoped” CsBa_2I_5 crystals reported in [17]. The decay curve for 500 nm emission is non-exponential and can be fitted using a bi-exponential function with decay constants of

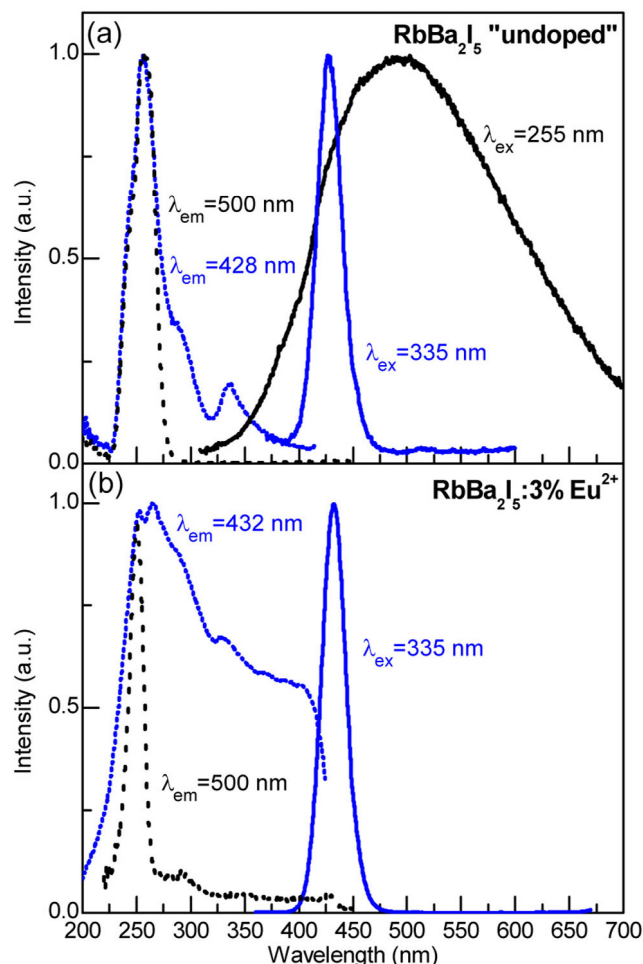


Fig. 4. Excitation and emission spectra of undoped RbBa_2I_5 (a) and $\text{RbBa}_2\text{I}_5:3\%\text{Eu}^{2+}$ (b) crystals at 300 K.

$\tau_1 = 255$ and $\tau_2 = 1095$ ns. However, these values are only estimates. For $\text{RbBa}_2\text{I}_5:3\%\text{Eu}^{2+}$, the main lifetime component of Eu^{2+} emission under photoexcitation is about 500 ns. The second long component of about 1100 ns can be associated with phosphorescence caused by optical filling and following depopulation of shallow traps.

X-ray excited decay curve of $\text{RbBa}_2\text{I}_5:3\%\text{Eu}$ is presented in Fig. 5c. Bi-exponential fitting gives decay constants of about 800 and 3600 ns. The main component of 800 ns (84%) is attributed to Eu^{2+} emission, whereas the presence of a long component (16%) can probably be associated with delayed recombination of charge carriers on lattice defects and/or uncontrolled impurities. The values obtained are close to 890 and 4800 ns lifetimes for $\text{RbSr}_2\text{I}_5:2.5\%\text{Eu}$ reported in [7].

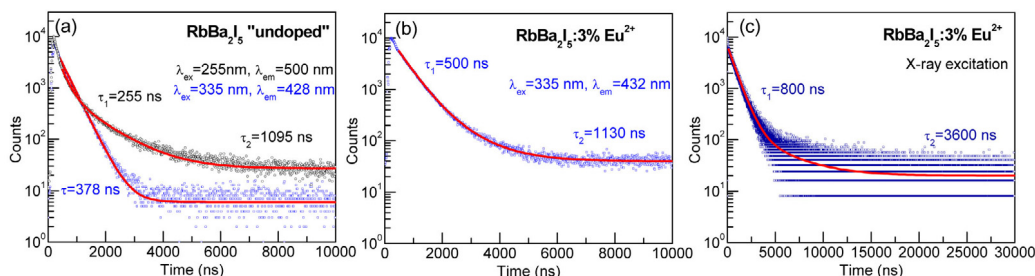


Fig. 5. Photoluminescence decay time profiles of undoped RbBa_2I_5 (a), $\text{RbBa}_2\text{I}_5:3\%\text{Eu}^{2+}$ (b) and X-ray excited decay curve of $\text{RbBa}_2\text{I}_5:3\%\text{Eu}$ (c) at 300 K.

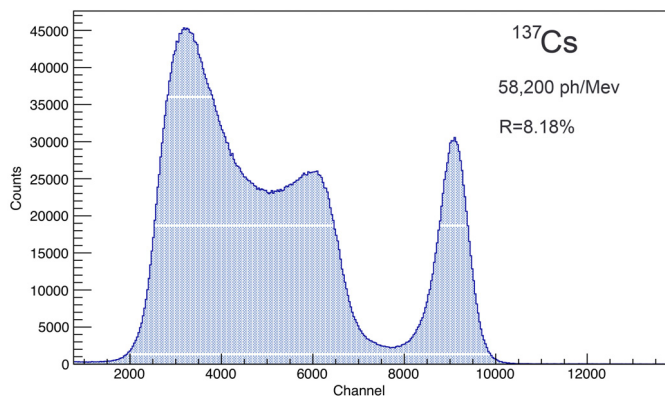


Fig. 6. Pulse height spectrum of the $\text{RbBa}_2\text{I}_5:3\%\text{Eu}^{2+}$ sample with a ^{137}Cs excitation source.

Fig. 6 shows the pulse height spectrum of the $\text{RbBa}_2\text{I}_5:3\%\text{Eu}^{2+}$ crystal when irradiated with a ^{137}Cs source (662 keV). The sample of $\text{RbBa}_2\text{I}_5:3\%\text{Eu}^{2+}$ exhibits a scintillation light output of $58,200 \pm 2900$ ph/MeV with energy resolution of $8.18 \pm 0.31\%$. Poor energy resolution is associated with low-quality crystal. To achieve a better energy resolution, our future work will be aimed at optimizing the concentration of Eu^{2+} and purification of the raw materials.

4. Conclusion

We present the luminescent and scintillation properties of the new bright $\text{RbBa}_2\text{I}_5:3\%\text{Eu}^{2+}$ scintillator grown by the Bridgman–Stockbarger technique in a sealed evacuated quartz ampoule coated with pyrolytic carbon. Our first results show that the $\text{RbBa}_2\text{I}_5:3\%\text{Eu}^{2+}$ crystal has a good scintillation light output 58,200 ph/MeV, and it is also less hygroscopic than NaI:Tl . The observed blue luminescence peaking at 436 nm with a main decay time of 800 ns is typical for the $4f^65d^1 \rightarrow 4f^7$ radiative transitions of Eu^{2+} ions. Moderate hygroscopicity, as well as a relatively high light yield and $Z_{\text{eff}} = 52.94$, allows us to consider this material as a potential candidate for use in radiation detection applications. Our further studies will be aimed at finding the optimal concentration of europium and improving the preparation of starting materials in order to eliminate the possible negative effect of uncontrolled impurities and defects on scintillation performance of $\text{RbBa}_2\text{I}_5:\text{Eu}^{2+}$ crystals.

CRediT authorship contribution statement

N.V. Rebrova: Conceptualization, Resources, Data curation, Writing - original draft. **A.Yu. Grippa:** Methodology, Investigation, Writing - original draft. **R. Calà:** Investigation, Writing - review & editing. **L. Martinazzoli:** Investigation, Writing - review & editing. **E. Auffray:** Investigation, Writing - review & editing. **I.A. Boiaryntseva:** Investigation, Writing - original draft, Visualization.

Declaration of competing interest

The authors declare that they have no known competing financial interests or personal relationships that could have appeared to influence the work reported in this paper.

Acknowledgments

This work was carried out in the frame of Crystal Clear Collaboration and supported by the National Academy of Sciences of Ukraine, under project No. 0119U100764 (“Development of high-efficiency scintillation inorganic materials for the new system of low-background nuclear spectrometry and medical diagnostics”). The authors would like to express fair gratitude to Mr. Valerii Kononets and Prof. Christophe Dujardin for assistance in research.

References

- [1] M. Moszynski, Inorganic scintillation detectors in γ -ray spectrometry, Nucl. Instrum. Methods Phys. Res. A 505 (2003) 101–110.
- [2] P. Dorenbos, J.T.M. de Haas, C.W.E. van Eijk, Non-proportionality in the scintillation response and the energy resolution obtainable with scintillation crystals, IEEE Trans. Nucl. Sci. 42 (1995) 2190–2202.
- [3] N.J. Cherepy, S.A. Payne, S.J. Asztalos, G. Hull, J.D. Kuntz, T. Niedermayr, S. Pimputkar, J.J. Roberts, R.D. Sanner, T.M. Tillotson, E. van Loef, C.M. Wilson, K.S. Shah, U.N. Roy, R. Hawrami, A. Burger, L.A. Boatner, Woon-Seng Choong, W.W. Moses, Scintillators with potential to supersede lanthanum bromide, IEEE Trans. Nucl. Sci. 56 (3) (2009) 873–880.
- [4] Z. Yan, G. Gundiah, G.A. Bizarri, E.C. Samulon, S.E. Derenzo, E. Bourret-Courchesne, Eu^{2+} -activated BaCl_2 , BaBr_2 and BaI_2 scintillators revisited, Nucl. Instrum. Methods Phys. Res. A 735 (2014) 83–87.
- [5] L.A. Boatner, J.O. Ramey, J.A. Kolopus, J.S. Neal, Divalent europium doped and undoped calcium iodide scintillators: Scintillator characterization and single crystal growth, Nucl. Instrum. Methods Phys. Res. A 786 (2015) 23–31.
- [6] L. Stand, M. Zhuravleva, G. Gamarda, A. Lindsey, J. Johnson, C. Hobbs, C.L. Melcher, Exploring growth conditions and Eu^{2+} concentration effects for $\text{K Sr}_2\text{I}_5:\text{Eu}$ scintillator crystals, J. Cryst. Growth 439 (2016) 93–98.
- [7] L. Stand, M. Zhuravleva, J. Johnson, M. Koschan, E. Lukosi, C.L. Melcher, New high performing scintillators: $\text{RbSr}_2\text{Br}_5:\text{Eu}$ and $\text{RbSr}_2\text{I}_5:\text{Eu}$, Opt. Mater. 73 (2017) 408–414.
- [8] H.J. Kim, H.S. Lee, H.C. Bhang, J.H. Choi, H. Dao, I.S. Hahn, M.J. Hwang, S.W. Jung, W.G. Kang, D.W. Kim, S.C. Kim, S.K. Kim, T.Y. Kim, Y.D. Kim, J.W. Kwak, Y.J. Kwon, J. Lee, J.H. Lee, J.I. Lee, M.J. Lee, M.H. Lee, J. Li, X. Li, S.S. Myung, S. Ryu, J.H. So, J.J. Zhu, Development of low background CsI(Tl) crystals and search for WIMP, IEEE Trans. Nucl. Sci. 55 (3) (2008) 1420–1424.
- [9] L. Stand, M. Zhuravleva, B. Chakoumakos, J. Johnson, A. Lindsey, C.L. Melcher, Scintillation properties of Eu^{2+} -doped KBa_2I_5 and K_2BaI_4 , J. Lumin. 169 (2016) 301–307.
- [10] G. Bizarri, E. Bourret-Courchesne, Z. Yan, S. Derenzo, Scintillation and optical properties of $\text{BaBrI}:\text{Eu}^{2+}$ and $\text{CsBa}_2\text{I}_5:\text{Eu}^{2+}$, IEEE Trans. Nucl. Sci. 58 (6) (2011) 3403–3410.
- [11] G. Meyer, G. Schilling, in: ICDD Grant in Aid, Institut für Anorganische Chemie, University Hannover, Germany, 1993.
- [12] G. Schilling, G. Meyer, Ternare Bromide und Iodide zweiwertiger Lanthanide und ihre Erdalkali-Analoga vom Typ AM_3X_5 und AM_2X_5 , Z. Anorg. Allg. Chem. 622 (1996) 759–765.
- [13] J.A. Smith, J.S. Kallman, H.E. Martz Jr., Case for an Improved Effectiva-Atomic-Number for the Electronic Baggage Scanning Program, LLNL-TR-520312-REV-1, Lawrence Livermore National Laboratory, Livermore, CA, USA, 2012, pp. 1–19, <http://dx.doi.org/10.2172/1055845>.
- [14] C. Kuntner, E. Auffray, P. Lecoq, C. Pizzolotto, M. Schneegans, Intrinsic energy resolution and lightoutput of the $\text{Lu(0:7)Y(0:3)AP}:\text{Ce}$ scintillator, Nucl. Instrum. Methods Phys. Res. A 493 (2002) 131–136.
- [15] O. J. Rubio, Doubly-valent rare-earth ions in halide crystals, J. Phys. Chem. Solids 52 (1991) 101–174.
- [16] J. Glodo, E.V. van Loef, N.J. Cherepy, S.A. Payne, C.M. Wilson, K.S. Shah, Concentration effects in Eu doped SrI_2 , IEEE Trans. Nucl. Sci. 57 (3) (2010) 1228–1232.
- [17] M.S. Alekhin, D.A. Biner, K.W. Krämer, P. Dorenbos, Optical and scintillation properties of $\text{CsBa}_2\text{I}_5:\text{Eu}^{2+}$, J. Lumin. 145 (2014) 723–728.
- [18] C.M. Fang, K. Biswas, Preferential Eu site occupation and its consequences in the ternary luminescent halides $\text{AB}_2\text{I}_5:\text{Eu}^{2+}$ ($A = \text{Li-Cs}$; $B = \text{Sr, Ba}$), Phys. Rev. A 4 (2015) 014012.
- [19] N.J. Cherepy, G. Hull, T.R. Niedermayr, A. Drobshoff, S.A. Payne, U.N. Roy, Y. Cui, A. Bhattacharya, M. Harrison, M. Guo, M. Groza, A. Burger, Barium iodide single-crystal scintillator detectors, in: Proceedings of the Society of Photo-Optical Instrumentation Engineers, San Diego, California, United States, 2007, 6706, 670616.